![OUKA — The University of Osaka Institutional Knowledge Archive](logo)

Title	Parameter Tuning of the Protocol Interference Model Using SINR for Time Slot Assignment in Wireless Mesh Networks
Author(s)	Kang, Gyeongyeon; Taniguchi, Yoshiaki; Hasegawa, Go et al.
Citation	IEICE Transactions on Information and Systems. 2011, E94-D(11), p. 2191-2200
Version Type	VoR
URL	https://hdl.handle.net/11094/23095
rights	Copyright © 2011 The Institute of Electronics, Information and Communication Engineers
Note	

PAPER

Parameter Tuning of the Protocol Interference Model Using SINR for Time Slot Assignment in Wireless Mesh Networks*

Gyeongyeon KANG[†a], *Nonmember*, **Yoshiaki TANIGUCHI**[††b], **Go HASEGAWA**[††c], *and* **Hirotaka NAKANO**[††d], *Members*

SUMMARY   In time division multiple access (TDMA)-based wireless mesh networks, interference relationships should be considered when time slots are assigned to links. In graph theory-based time slot assignment algorithms, the protocol interference model is widely used to determine radio interference information, although it is an inaccurate model of actual radio interference. On the other hand, the signal-to-interference-plus-noise-ratio model (SINR model) gives more accurate interference relationships but is difficult to apply to time slot assignment algorithms since the radio interference information cannot be determined before time slot assignment. In this paper, we investigate the effect of the parameters of the protocol interference model on the accuracy of the interference relationships determined using this model. Specifically, after assigning time slots to links based on the protocol interference model with various interference ratios, which is the major parameter of the protocol interference model, we compare the interference relationship among links in the protocol interference and SINR models. Through simulation experiments, we show that accuracy of the protocol interference model is improved by up to 15% by adjusting the interference ratios of the protocol interference model.
key words: *wireless mesh networks, protocol interference model, SINR model, TDMA, parameter tuning*

1. Introduction

Wireless mesh networks for providing wireless broadband access have attracted a great deal of attention because of their expandability and cost efficiency [2]. Wireless mesh networks consist of a gateway node, which is connected to a wired network, and mesh nodes as shown in Fig. 1. A mesh node provides a wireless broadband access service to client terminals within its service area. Mesh nodes are connected through a wireless link when they are within transmission range of each other. A wireless mesh network is also called a wireless relay network when the topology is a tree.

When closely located links in a wireless network are used simultaneously, a receiver node cannot correctly receive radio signals from the corresponding sender node due to *radio interference*, which is why it is necessary to avoid

radio interference in wireless networks. Time division multiple access (TDMA) is a fundamental technique for avoiding radio interference. In TDMA protocols, time is divided into frames, each of which consists of time slots of constant duration. Different time slots are then assigned to links that interfere with each other. The performance of TDMA-based wireless mesh networks is highly dependent on the time slot assignment algorithms. Until now, graph theory-based time slot assignment algorithms have been studied [3]–[8] because time slot assignment algorithms can be analogous to graph coloring.

Graph theory-based time slot assignment algorithms require information about the interference relationships among links before assigning time slots to links. In these algorithms, the *protocol interference model* (a.k.a. the unified disk graph model or ratio-K model) [9] has been widely used to obtain radio interference information [4], [8]. In the protocol interference model, the radio interference range is defined as a circle centered on a sender node. The radius of an interference range is determined by the *interference ratio* parameter. Since the interference relationships among links are defined according to the location and interference ranges of nodes, the protocol interference model can be easily used in theoretical analysis. However, the protocol interference model is not an accurate model of actual radio interference [10]. For example, close links can be used simultaneously when each receiver node can receive signals of sufficient strength from the corresponding sender node, even if the protocol interference model indicates that the links interfere with each other [11]. This is called the capture effect. In addition, there are situations in which a receiver node cannot correctly receive radio signals from a sender node when many links are used simultaneously and interfere with the
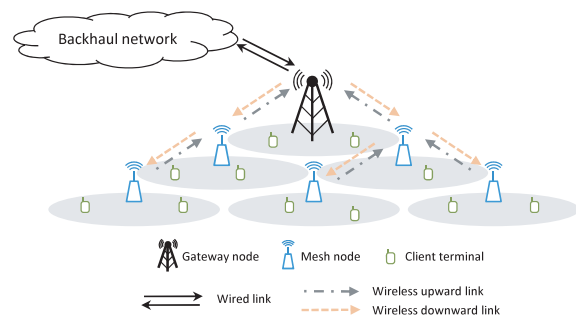

Fig. 1   A wireless mesh network.

receiver node, even if there are no interference relationships among the links in the protocol interference model.

To apply graph theory-based time slot assignment algorithms to actual wireless mesh networks, accurate information on interference relationships is needed in order to avoid interference among links and to assign time slots to links efficiently. In other words, accurate radio interference models are needed that can be applied in graph theory-based time slot assignment algorithms.

Among the radio interference models, the *signal-to-interference-plus-noise ratio (SINR) model* [10], [12] is known for its accurate representation of radio interference. In this model, the received signal strength is first obtained, and then the SINR is calculated. When the SINR of a link is above a certain threshold value, the receiver node can successfully receive the radio signal from the sender node. The SINR model can handle features of actual wireless radio propagation such as Rayleigh fading, shadowing effects and capture effects [12], [13]. However, to determine interference relationships among links, the SINR model requires information not only on the locations of the sender and receiver nodes but also on other nodes that simultaneously emit radio signals. Therefore, radio interference information cannot be determined before assigning time slots to links, and the SINR model cannot be applied directly in graph theory-based time slot assignment algorithms.

In this paper, to apply graph theory-based time slot assignment algorithms, we obtain a more accurate radio interference model by adjusting the interference ratio parameter of the protocol interference model according to the SINR. By obtaining a more accurate protocol interference model, interference among links can be avoided and time slots can be assigned to links efficiently without modification of the graph theory-based time slot assignment algorithms. For this purpose, we investigate the effect of varying parameters of the protocol interference model on the accuracy of predicted interference relationships. Specifically, after assigning time slots to links based on the protocol interference model with various interference ratios, we compare the interference relationships among links for the protocol interference and SINR models. To adjust the interference ratio parameter, we propose three heuristic methods, each of which selects different nodes as candidates for interference ratio adjustment. The effectiveness of the parameter adjustment methods are evaluated through simulation experiments in terms of accuracy of interference decision and network performance which is result of time slot assignment.

The rest of this paper is organized as follows. In Sect. 2, we introduce some related studies. In Sect. 3, we explain the wireless mesh network model, the protocol interference model and the time slot assignment algorithm which are used in this paper. Then in Sect. 4, we explain the SINR model and propose three methods for adjusting the interference ratio in the protocol interference model using the SINR. We investigate the effects of parameters in the protocol interference model with our proposed interference adjustment methods through simulation experiments in Sect. 5.

Finally, we give conclusions and discuss future work in Sect. 6.

2. Related Work

2.1 Graph Theory-Based Time Slot Assignment Algorithms

In the past literature, there have been proposed many graph theory-based time slot assignment algorithms for wireless networks [3]–[8], because time slot assignment algorithms can be analogous to conflict graph coloring. Clark et al. have shown that coloring with minimum sum of colors for an arbitrary graph is a NP-hard problem [3]. Then they propose a greedy coloring algorithm. In the algorithm, each link is allocated the earlier time slots from the beginning of a frame by avoiding interference. Kumar et al. have proposed a distributed time slot assignment algorithm which incorporates fairness, energy and path-length requirements [5]. Wang et al. have proposed some time slot assignment algorithms for decreasing the frame length [7]. Their algorithms handle different transmission ranges and different interference ranges among nodes. Ishii et al. have extended the algorithms in [7] to accommodate weighted time slot assignment and to reduce transmission latency [8].

These graph theory-based time slot assignment algorithms require information about the interference relationships among links before assigning time slots to links. The information on interference relationships should be accurate to avoid interference among links and to assign time slots to links efficiently. Our proposal in this paper can be applied to these graph theory-based time slot assignment algorithms without modification of the algorithms.

2.2 Interference Models

In addition to the protocol interference and SINR models there are a variety of radio interference models for wireless networks. The *request to send / clear to send (RTS/CTS) interference model* [4], [14] is a radio interference model based on the RTS/CTS flow control which is widely used in carrier sense multiple access (CSMA) mechanisms. In the RTS/CTS interference model, both the receiver node and the sender node have circular radio interference ranges, whereas only the sender node has a radio interference range in the protocol interference model. In the *hop-based interference model* [15], [16], a sender node interferes with other links whose receiver node is within a certain number of hops from the sender node. This model is widely used in practical wireless network protocols. The *sender-based interference model* [17] is similar to the protocol interference model. In this model, a sender node interferes with all links whose receiver or sender nodes are within the interference range of the sender node. The sender-based interference model can be easily used to analyze wireless networks. The *link quality-based interference model* [18] is a measurement-based radio interference model. In this model,

interference relationships are determined according to the packet reception rate among links.

The SINR model is classified into two models according to the way to obtain the received signal strength. In this paper, we call the two models as the *measurement-based SINR model* and the *equation-based SINR model*. In the measurement-based SINR model, the received signal strength for each node pair is at first measured. Then SINR is calculated using the measured received signal strength values. The measurement-based SINR model can be accomplished accurate representation of radio interference, however, preliminary measurements for each received signal strength are required to use the model for time slot assignment algorithms. Some studies are based on the measurement-based SINR model [18], [19]. On the other hand, in the equation-based SINR model, the received signal strength is calculated from equations with some parameters. The SINR is then calculated using the calculated received signal strength. The equation-based SINR model is suitable for analysis and simulation evaluations. Some studies are based on the equation-based SINR model [9], [12], [19].

The radio interference models have been compared in previous studies [10], [18]–[20]. Maheshwari et al. have investigated the accuracy of radio interference models in IEEE 802.15.4-based wireless sensor networks [18]. They conducted experiments using 20 TelosB commercial sensor nodes, and evaluated the accuracy of the protocol interference model, the measurement-based SINR model, the hop-based interference model, the link quality-based interference model and the range-based interference model. They found that the measurement-based SINR model is the most accurate predictor of radio interference. Furthermore, they evaluated the throughput of the wireless sensor network using a time slot assignment algorithm based on each radio interference model. Through experimental evaluations, they demonstrated that time slot assignment based on the measurement-based SINR model achieves the highest throughput.

Zhu and Lu have compared a physical radio interference model and the hop-based interference model, which is used in IEEE 802.16 wireless mesh networks [20]. Through simulation evaluations using a QualNet simulator, it was shown that about 7% of links cannot be used due to radio interference when we assume that there are interference relationships among links within three-hop links in the hop-based interference model.

Shi et al. have compared the protocol interference model and the SINR model for multi-hop multi-channel wireless ad hoc networks to determine how to use the protocol interference model correctly [10]. They show that the link capacity of wireless networks based on the protocol interference model can be close to that based on the SINR model by using an appropriate parameter value for all nodes in the protocol interference model. Che et al. also have compared the protocol interference and SINR models for mission-critical wireless networks [19]. They proposed the physical-ratio-K (PRK) interference model, which is combination of the protocol interference and SINR models, and showed that the throughput of a wireless network based on the PRK interference model is close to that of one based on the SINR model while ensuring the required packet delivery reliability. They used the equation-based SINR model for analysis, and the measurement-based SINR model for the testbed experiments.

In this paper, we also compare the protocol interference and SINR models. In contrast to [10], [19], the purpose of our study is to use the protocol interference model for graph theory-based time slot assignment algorithms in TDMA-based wireless mesh networks. To use the protocol interference model correctly, we consider an adjustment of the interference ratio parameter of the protocol interference model for each node. In addition, we conduct detailed a comparison of the protocol interference and SINR models. We compare the accuracy of interference prediction for the protocol interference model and the SINR model, whereas the previous studies [10], [19] have only compared the performance of wireless networks. To evaluate fundamental performance of our proposal through simulation evaluations while changing parameters and topologies, we use the equation-based SINR model in this paper. Hereinafter, we simply denote the equation-based SINR model as SINR model. Testbed-based evaluations using the measurement-based SINR model are future work.

3. System Model

In this section, we briefly explain the wireless mesh network model and the time slot assignment algorithm which are assumed in this paper. We consider the same wireless mesh network that is used by Ishii et al. [8].

3.1 Wireless Mesh Network Model

We assume that there is a set of n mesh nodes $\mathcal{V} = \{v_1, v_2, \ldots, v_n\}$ deployed in a plane. We consider the directed communication graph $\mathcal{G}^c = (\mathcal{V}, \mathcal{E}^c)$ which gives the communication relationships for each node. $\mathcal{E}^c$ is the set of directed communication links $l_{i,j}$, representing a link directed from mesh node $v_i \in \mathcal{V}$ to mesh node $v_j \in \mathcal{V}$. The existence of directed communication link $l_{i,j}$ in the graph $\mathcal{G}^c$ is determined according to the protocol interference model which is described later. One of the mesh nodes is the gateway node that is connected to a wired network, and we assume, without loss of generality, that mesh node v_1 is the gateway node. Figure 2 (a) shows an example of directed communication graph where eleven mesh nodes and a gateway node are deployed on a flat region. In the figure, a filled circle, an open circle and an arrow line indicate a gateway node, a mesh node and a directed communication link, respectively.

There are two types of communication: upward communication and downward communication. In upward communication, data is transferred from mesh nodes toward the gateway node. Conversely, data is transferred from the gate-
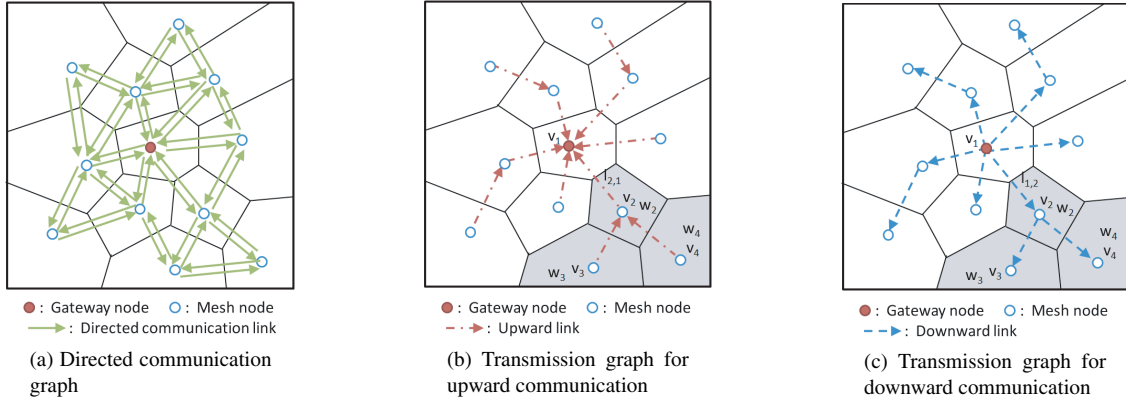
Fig. 2 Example of a wireless mesh network.

(a) Directed communication graph

(b) Transmission graph for upward communication

(c) Transmission graph for downward communication

way node toward mesh nodes in downward communication. Communication between the gateway node and mesh nodes is achieved through intermediate mesh nodes in a multi-hop fashion along a path is determined by a routing algorithm. In this paper, we consider a tree-based routing algorithm which constructs the transmission graphs for upward communication, $\mathcal{G}^t_{up} = (\mathcal{V}, \mathcal{E}^t_{up})$, and downward communication, $\mathcal{G}^t_{dw} = (\mathcal{V}, \mathcal{E}^t_{dw})$, as tree graphs. Here, $\mathcal{E}^t_{up} \subset \mathcal{E}^c$ and $\mathcal{E}^t_{dw} \subset \mathcal{E}^c$. In the transmission graphs, the root is the gateway node and each node is connected to the gateway node through minimum-hop and minimum-distance links. We call the link $l_{i,j} \in \mathcal{E}^t$ in $\mathcal{G}^t$ a transmission link, where $\mathcal{E}^t \in \{\mathcal{E}^t_{up}, \mathcal{E}^t_{dw}\}$ and $\mathcal{G}^t \in \{\mathcal{G}^t_{up}, \mathcal{G}^t_{dw}\}$. In addition, a link that is on a path directed toward the gateway node is called an upward link, and a link that is on a path directed away from the gateway node is called a downward link. Figures 2 (b) and 2 (c) show examples of transmission graphs for upward and downward communication, respectively. The transmission links are determined by the routing algorithm and the directed communication graph shown in Fig. 2 (a).

The traffic demand w_i between mesh node v_i and client terminals is determined in proportion to the size of the Voronoi cell [21] of mesh node v_i in both upward and downward communication. Here, an intermediate mesh node relays data from a child node to a parent node in upward communication, and it relays data from a parent node to a child node in downward communication. Therefore, the traffic load of a mesh node becomes the sum of the traffic demands of mesh nodes that are within the subtree whose root is the mesh node. For example, each cell with a solid line boundary in Fig. 2 is a Voronoi cell, and each traffic demand between a mesh node and client terminals is determined according to the Voronoi cell. When mesh node v_2 transfers data to the gateway node v_1 using upward link $l_{2,1}$ in upward communication, the traffic load of upward link $l_{2,1}$ becomes the sum of traffic demands w_2, w_3 and w_4, whose Voronoi cells are shown as shaded areas in Fig. 2 (b). In a similar fashion, when the gateway node v_1 transfers data to mesh node v_2 using downward link $l_{1,2}$ in downward communication, the traffic load of downward link $l_{1,2}$ becomes the sum of w_2, w_3 and w_4, as shown in Fig. 2 (c).
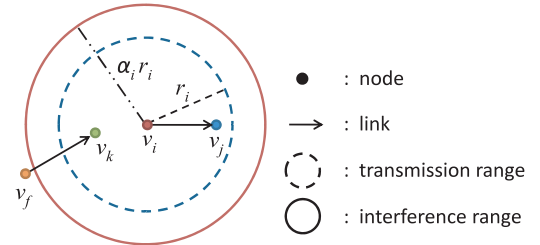

Fig. 3 Example of the behavior of the protocol interference model.

3.2 Interference Decisions in the Protocol Interference Model

In the protocol interference model [9], the existence of links and interference relationships between links are determined according to the location of node v_i, transmission radius r_i and interference ratio α_i as follows. When two nodes $v_i, v_j \in \mathcal{V}$ satisfy $\|v_i - v_j\| < r_i$, where $\|v_i - v_j\|$ stands for the distance between node v_i and node v_j, communication from sender node v_i to receiver node v_j is possible, and the directed communication link $l_{i,j} \in \mathcal{E}^c$ exists. In addition, sender node v_i interferes with a link whose receiver node v_k satisfies $\|v_i - v_k\| < \alpha_i r_i$. The interference ratio α_i is usually set at between 2 and 4 depending on the environment [7].

Figure 3 shows an example of an interference decision in the protocol interference model where there are two transmission links, $l_{i,j}$ and $l_{f,k}$. In this example, link $l_{i,j}$ interferes with link $l_{f,k}$ since receiver node v_k of link $l_{f,k}$ is within the interference range of link $l_{i,j}$.

3.3 Time Slot Assignment

In this paper, TDMA is adopted as the medium access control (MAC) protocol of the wireless mesh networks. In TDMA, time is divided into slots $\mathcal{T} = \{t_1, t_2, \ldots, t_m\}$, and different time slots are assigned to links which have an interference relationship. We call the total number of time slots, m, the frame length. The frame length can be reduced by the sharing of time slots by multiple links which do not interfere

with each other, which is called spatial reuse [22]. The interference relationships among the links are determined by the protocol interference model as described in Sect. 3.2.

For the time slot assignment algorithm at the transmission link, we adopt the greedy algorithm that was used by Ishii et al. [8]. In this time slot assignment algorithm, the order of time slot assignment for each transmission link is first determined according to the interference relationships among transmission links and the traffic load. Then, time slots are assigned to the transmission links avoiding interferences in a greedy manner. For each transmission link, a number of time slots whose number is determined according to the traffic load, are assigned. The frame length m is then the number of time slots, which depends on the deployment of mesh nodes and the interference relationships among transmission links.

4. Adjusting the Interference Ratio Parameter of Protocol Interference Model Using the SINR

The result of time slot assignment in the wireless mesh networks depends on the parameters of the protocol interference model. To apply the time slot assignment algorithm to real networks, the parameters should be configured to increase the accuracy of the interference decision. In this paper, we investigate the effect of the parameters of the protocol interference model on the accuracy in determining interference relationships. To evaluate the accuracy of interference decisions, we use the SINR model which gives a more accurate interference relationship. The parameter of the protocol interference model that we adjust is the interference ratio. In this section, we first explain the SINR model. Then, we propose methods for adjusting the interference ratio of the protocol interference model based on the SINR.

4.1 Interference Evaluation by the SINR Model

After assigning time slots to links by the time slot assignment algorithm, it is possible to evaluate the interference relationships among links using the SINR model. Let sender node and receiver node be v_i and v_j. We denote the communication period of link $l_{i,j}$ at time slot t_x by $c_{i,j,x}$ if time slot t_x is assigned to link $l_{i,j}$. In addition, let $\mathcal{V}^{int}_{i,j,x}$ be the set of sender nodes other than node v_i that use the same time slot as link $l_{i,j}$. The SINR $s_{i,j,x}$ during communication period $c_{i,j,x}$ is given by

$$s_{i,j,x} = \frac{p_{i,j}}{p_{noise} + \sum_{v_k \in \mathcal{V}^{int}_{i,j,x}} p_{k,j}} \tag{1}$$

where p_{noise} is the signal strength of noise, which depends on the environment. The strength of the signal received at node v_j from sender node v_i, $p_{i,j}$, is given by

$$p_{i,j} = R^2 e^\xi K \frac{p_i^{tr}}{\|v_i - v_j\|^\eta}. \tag{2}$$

Here, p_i^{tr} is the transmission power of the wireless signal

at sender node v_i, R is a random variable that follows a Rayleigh distribution to take into account Rayleigh fading, ξ is a parameter for considering shadowing effects, and K and η are parameters controlling power decay due to distance. The parameter η is usually set at between 2 and 4 depending on the environment [12].

In the SINR model, when $s_{i,j,x} \geq B$, the receiver node v_j can successfully receive radio signals from sender node v_i in communication period $c_{i,j,x}$. B is called the capture threshold which depends on the wireless devices used. On the other hand, when $s_{i,j,x}$ is less than threshold B, communication from sender node v_i to receiver node v_j fails in communication period $c_{i,j,x}$. This means that the set of sender nodes $\mathcal{V}^{int}_{i,j,x}$ interferes with link $l_{i,j}$.

4.2 Interference Ratio Adjustment Methods

After assigning time slot to links based on the protocol interference model with various interference ratios, we can compare the interference relationships among links to those based on the SINR model. In this subsection, we propose methods for adjusting the interference ratio of the protocol interference model based on the SINR model.

The SINR model cannot ensure that all SINRs in all communication periods exceed a certain threshold, since the SINR includes random variables as described in the previous subsection. In addition, in some wireless devices which employ adaptive modulation and coding (AMC) mechanisms, communication performance parameters, such as bit rate, change depending on the SINR. Therefore, a viewpoint that the SINR should exceed a certain threshold in a certain proportion of communication periods is meaningful, and we adjust the interference ratio of the protocol interference model to ensure that the SINR is greater than B in a proportion z ($0 < z \leq 1$) of all communication periods $C = \{c_{i,j,x}|l_{i,j} \in \mathcal{E}^t, t_x \in \mathcal{T}\}$.

Figure 4 shows the flowchart of the proposed method for adjusting the interference ratio. First, a transmission
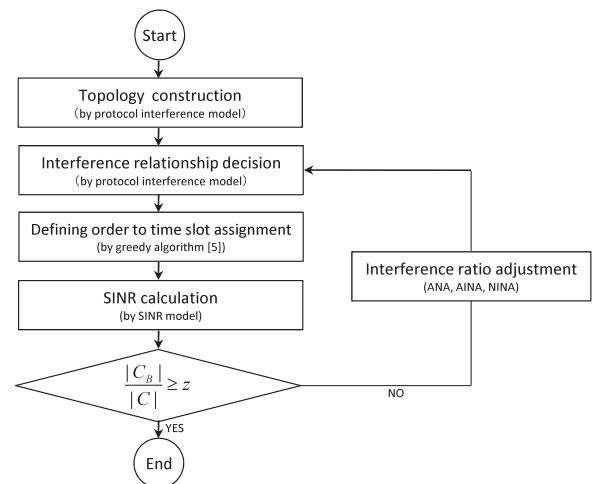

Fig. 4 Flowchart for adjusting the interference ratio.

graph $\mathcal{G}^t$ is generated based on the protocol interference model. Information on interference relationships among transmission links are then determined based on the protocol interference model, where the interference ratio of all nodes is set to an initial value α_0 that is assumed to be small. Next, a set of communication periods $C_B = \{c_{i,j,x} | s_{i,j,x} \geq B, c_{i,j,x} \in C\}$ is calculated using the SINR model. Then, if the inequality

$$\frac{|C_B|}{|C|} \geq z \tag{3}$$

is satisfied, the interference ratio adjustment is finished. On the other hand, if the inequality is not satisfied, we adjust the interference ratio as described in a later subsection. Then we again determine the interference relationships among transmission links and assign time slots based on the protocol interference model. This process is repeated until Eq. (3) is satisfied. In the next three subsections, we propose three heuristic methods for adjusting the interference ratio parameter, each of which selects different nodes as candidates for interference ratio adjustment.

4.2.1 All Nodes Adjustment (ANA) Method

In the ANA method, the interference ratio α_i of all nodes is adjusted by adding δ. Figure 5 shows an example transmission graph for the case of eight nodes and seven transmission links. Let transmission link $l_{7,4}$ have the minimum SINR $s_{min} = \min\{s_{i,j,x} | c_{i,j,x} \in C\}$ in time slot t_w. In addition, let the time slot t_w be assigned to transmission links $l_{8,1}$, $l_{7,4}$, $l_{6,5}$ and $l_{3,2}$. In the ANA method, the interference ratios of all nodes, that is, v_1–v_8, are adjusted.

The ANA method is simple and increases the interference ratio of all nodes even if there is no difference between the results of the interference decision in the protocol interference model and the SINR model in a local region. If the interference ratio is increased more than necessary, more links are considered to have interference relationships, and the number of time slots increases.

4.2.2 All Interference Nodes Adjustment (AINA) Method

In the AINA method, the interference ratio is adjusted locally. Let the SINR in communication period $c_{g,h,w}$ be the minimum SINR s_{min}, and let the set of sender nodes which give interference to transmission link $l_{g,h}$ be $\mathcal{V}^{int}_{g,h,w}$. At transmission link $l_{g,h}$, there is the largest difference between the
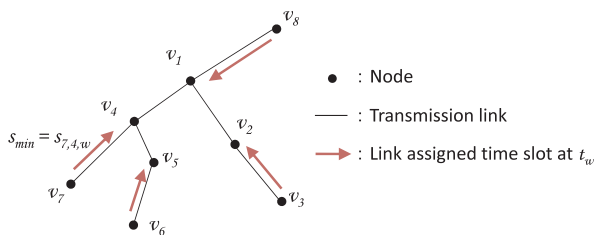

Fig. 5   Example of a transmission graph.

resulting interference relationships in the protocol interference and SINR models. The AINA method adjusts the interference ratio of all nodes in $\mathcal{V}^{int}_{g,h,w}$ by adding δ. In the example of Fig. 5, the interference ratio of sender nodes $\mathcal{V}^{int}_{7,4,w} = \{v_3, v_6, v_8\}$, which are assigned the same time slot as transmission link $l_{7,4}$, are adjusted.

The AINA method adjusts the interference ratio of all sender nodes within $\mathcal{V}^{int}_{g,h,w}$. Therefore, it may increase the interference ratio of a node more than necessary when the node is far enough from the receiver node v_h that has the minimum SINR.

4.2.3 Nearest Interference Node Adjustment (NINA) Method

In the NINA method, the interference ratio of the node that is the closest to the receiver node v_h, among the set of nodes $\mathcal{V}^{int}_{g,w}$, is adjusted by adding δ. In Fig. 5, node v_6 is the nearest to receiver node v_4 among the set of nodes $\mathcal{V}^{int}_{7,4,w}$, and so its interference ratio is adjusted.

5. Simulation Experiments

In this section, we evaluate the protocol interference model with the proposed interference ratio adjustment methods through simulation experiments.

5.1 Evaluation Environment

We use an IEEE 802.16j mesh network simulator developed in our laboratory. In the simulation, one gateway node is placed at the center and 49 nodes are randomly distributed in a 1×1 square area. We use the protocol interference model to obtain interference relationship information before time slot assignment, and the SINR model to adjust the interference ratio parameter using our proposed methods as described in previous sections. In the protocol interference model, the transmission distance r_i is set to 0.18 for all nodes. In the SINR model, the transmission power p^{tr}_i and the parameter of power decay η are set to 1.0 and 3.0, respectively. Environmental noise p_{noise} is set to 32, which is same level as the case that there are four sender nodes at a distance of 0.5 from the receiver node. Other parameters e^ξ, K and R in Eq. (2) are set to 1.0, which mean that there is no Rayleigh fading and shadowing effects. The initial interference ratio α_0 and the incremental ratio δ are set to 0.0 and 0.01, respectively. As the interference model of the simulator, we also use same SINR model to evaluate fundamental comparative evaluation between the SINR model and the protocol interference model with our proposed methods.

In this paper, the *false negative rate* and the *false positive rate* are used to measure the accuracy of the interference decision in the protocol interference model. We define them as follows. First, we consider the set $\mathcal{Y}$ which is the set of transmission links that become candidates to be assigned same time slot. Here, we should note that we exclude sets

of transmission links where neighboring links are simultaneously selected, since we assume a single channel is used in the wireless mesh network. Therefore, $\mathcal{Y}$ is the set

$$\mathcal{Y} = \{X | X \subset \mathcal{E}, X \neq \emptyset,$$
$$\forall l_{i,j} \forall l_{m,n} (l_{i,j} \in X, l_{m,n} \in X, i \neq m,$$
$$j \neq n, i \neq n, j \neq m, l_{i,j} \neq l_{m,n})\}. \quad (4)$$

For any set of transmission links in $\mathcal{Y}$, interference relationships can be determined by the protocol interference model and the SINR model. If there is an interference relationship in a set of transmission links, the transmission links cannot be used simultaneously. Therefore, a set of transmission links in $\mathcal{Y}$ can be classified to belong to one of four cases. When both the SINR model and the proposed protocol interference model agree on whether or not a set of transmission links can be successfully used simultaneously, the set of transmission links is classified as true positive or true negative. When the SINR model produces the result that a set of transmission links can be used simultaneously and the proposed model produces the result that the set of transmission links cannot be used simultaneously, the set of transmission links is classified as false negative. In the opposite case, it is classified as false positive. We denote the number of true positives, false negatives, false positives and true negatives by N_{tp}, N_{fn}, N_{fp} and N_{tn}, respectively. The false positive rate R_{fp} and the false negative rate R_{fn} are given by

$$R_{fn} = \frac{N_{fn}}{N_{tp} + N_{fn}}, \quad (5)$$

$$R_{fp} = \frac{N_{fp}}{N_{fp} + N_{tn}}. \quad (6)$$

When the false positive rate and the false negative rate are close to zero, it means that the protocol interference model is highly accurate.

As evaluation metrics of network performance, we use the *number of time slots* and the *gateway throughput*. The former metric is the number of time slots assigned by the time slot assignment algorithm [8], and indicates the efficiency of spatial reuse. Fewer time slots mean higher efficiency of spatial reuse. The gateway throughput is the number of time slots assigned to the gateway node in a frame, and it represents the communication efficiency between the wireless mesh network and the external wired network. A higher gateway throughput means higher network communication efficiency. In this paper, to evaluate fundamental network performance, we do not consider situations where network performance varies for each time slot. That is, we do not consider AMC mechanisms and random conditions of radio propagation such as Rayleigh fading in the simulation experiments. Therefore, the number of time slots and the gateway throughput can be evaluated when $z = 1.0$.

For comparison, we also conduct simulations where a SINR-based time slot assignment algorithm is used (hereinafter referred to as SINR coloring). SINR coloring assigns time slots to transmission links in an order that is determined by the time slot assignment algorithm. If the SINR of all

transmission links will be over the threshold B, the current time slot is assigned to the transmission link; otherwise, a new time slot is assigned to the transmission link. Here, we should note that SINR coloring is modification of the time slot assignment algorithm [8] considering the SINR model. The purpose of this paper is to obtain an accurate interference model that can be applied in graph theory-based time slot assignment algorithms as described in Sect. 1. Therefore, the direct comparison between the graph theory-based time slot assignment algorithm based on the protocol interference model with our proposed interference ratio adjustment methods and SINR coloring is not adequate. In addition, since SINR coloring is one of time slot assignment algorithms, evaluation of accuracy of the protocol interference model, that is, the false negative rate and the false positive rate, cannot be conducted. SINR coloring improves the network performance compared to the graph theory-based time slot assignment algorithm with the protocol interference model, since SINR coloring assigns time slots to links according to the SINR model which is an accurate interference model compared to the protocol interference model. In this paper, we use SINR coloring as a reference method to achieve an upper bound of the performance of the graph theory-based time slot assignment method based on the protocol interference model with our proposed methods.

In the following, the results are averaged over 100 topologies excluding the cases of disconnected graphs.

5.2 Evaluation of the Accuracy of the Protocol Interference Model

Figure 6 shows the false positive rate and the false negative rate of the protocol interference model with 99% confidence intervals when $z = 1.0$ and $B = 3$ dB. For comparison purposes, we also show the results for the protocol interference model where α is set to 2, 3 or 4. We refer to this as the *conventional method*. It can be seen in Fig. 6 that the false positive rate is larger and the false negative rate is smaller for the proposed methods than for the conventional method in both upward and downward communication. The reason for this is as follows. In the proposed methods, the interference ratios of the nodes are set to minimize the radio interference in the SINR model under a given topology and time slot assignment. Therefore, a lot of nodes have a smaller interference ratio compared with the conventional method. When a smaller interference ratio is used in the protocol interference model, more combinations of links are determined to have no interference relationship. That is, the number of sets of links which can be used simultaneously in the protocol interference model increases. Therefore, the number of true positives and the number of false positives increase. As a result, the false positive rate for the proposed methods becomes higher and the false negative rate for the proposed methods becomes lower compared with conventional method.

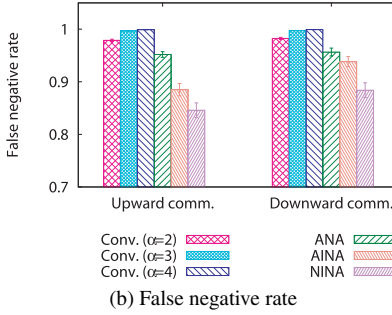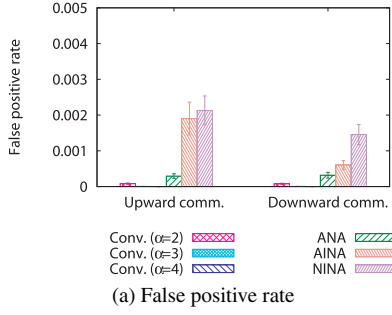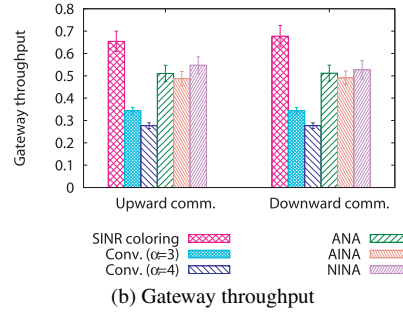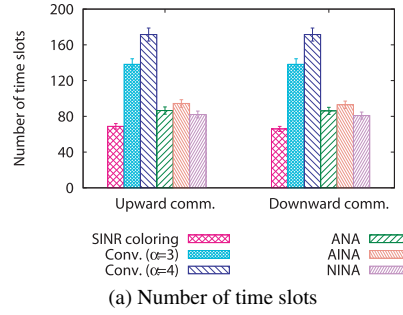Among the proposed methods, the NINA method shows the highest false positive rate and the lowest false

(a) False positive rate

(b) False negative rate

Fig. 6 Accuracy (z=1.0).

(a) Number of time slots

(b) Gateway throughput

Fig. 7 Network performance (z=1.0).

(a) Accuracy against z

(b) Accuracy against threshold B
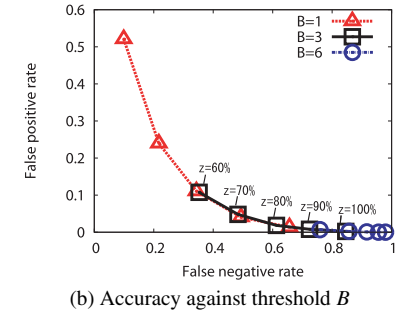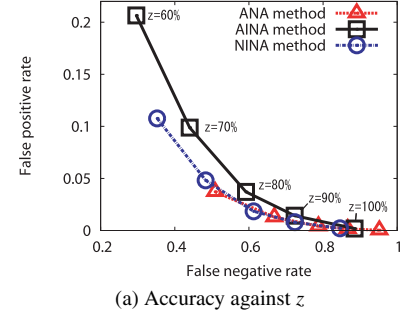
Fig. 8 Accuracy for various parameter values.

negative rate, while the ANA method exhibits the lowest false positive rate and the highest false negative rate. The reason for this is as follows. Both the AINA method and the NINA method adjust the interference ratio locally, whereas the ANA method increases the interference ratio of all nodes. Therefore, in the AINA and NINA methods, a lot of nodes are assigned the initial ratio or smaller interference ratios than in the ANA method. As a result, the false positive rate becomes higher and the false negative rate becomes lower for the AINA and NINA methods than for the ANA method. In addition, the NINA method is designed not to increase the interference ratio more than necessary compared with the AINA method. That is why the NINA method achieves the highest false positive rate and the lowest false negative rate.

Although the false positive rate for the NINA method is the highest, it is quite low at only 0.0022. On the other hand, the false negative rate for the ANA method decreases to 0.05, and that for the NINA method decreases to 0.15 compared with the conventional method which has the false negative rate of around 1.00. That is, the accuracy of the protocol interference model with the NINA method is improved by up to 15%. However, the false negative rate for the NINA method is still high, and is about 0.84 for upward communication. This is due to the limitation of the protocol interference model which employs a binary decision for the existence of radio interference based on a circular region.

When we compare the results of the AINA and NINA methods for upward and downward communication, the values are slightly different as shown Fig. 6. In this paper, since we assume a tree topology whose root is the gateway node of the wireless mesh network, the number of sender nodes and the density of receiver nodes in upward communication is larger than it is in downward communication. For ex-

ample, leaf nodes become only sender nodes in the case of upward communication. Therefore, the number of sets of links which can be used simultaneously in the SINR model decreases in upward communication. As a result, the number of false positives and the number of true negatives increase, and the false positive rate becomes higher in upward communication. Since there is a trade-off between the false positive rate and the false negative rate, the false negative rate decreases in upward communication.

5.3 Evaluation of the Network Performance

Figure 7 shows the average number of time slots and the average gateway throughput with 99% confidence intervals. Since there are links that cannot be used simultaneously under the SINR model when we use the conventional method with $\alpha = 2$, we only show results for the conventional method where α is set to 3 or 4. Here, we should note that the number of time slots is larger than the number of transmission links since a number of time slots are assigned for each transmission links according to the traffic load as described in Sect. 3.3.

As shown in Fig. 7, both the number of time slots and the gateway throughput of the proposed methods are drastically closer to the results for SINR coloring than the conventional methods. Among the proposed methods, the results for the NINA method are the closest to the results for SINR coloring. Because the accuracy of the protocol interference model with the NINA method is the highest, as described in the previous subsection, time slots are efficiently assigned to the links and communication efficiency becomes higher. As a result, the number of time slots with the NINA method is reduced by up to 5% compared to that with the ANA method and is reduced by up to 13% compared to that

with the AINA method on average. In addition, the gateway throughput with the NINA method is improved by up to 7% compared to that with the ANA method and is improved by up to 12% compared to that with the AINA method on average.

When we compare the number of time slots and the gateway throughput for upward and downward communication, the results are almost same.

5.4 Evaluation of the Accuracy for Various Parameter Values

As described in Sect. 5.2, the false negative rate of the protocol interference model is high although the false positive rate is low when $z = 1.0$. To evaluate the accuracy of the protocol interference model when the false negative rate is lower, we also conduct simulation evaluations under $z < 1.0$ in this section.

Figure 8 (a) shows the false positive rate and the false negative rate of the protocol interference model with the proposed methods when z is varied from 0.6 to 1.0. In the figure, the value of z is shown only next to the results of the AINA method. As we can see in Fig. 8 (a), there is a trade-off between false positive rate and false negative rate. For all the proposed methods the false negative rate becomes higher and the false positive rate becomes lower when z increases. This is because the interference ratio of nodes becomes smaller as z decreases since the number of iteration steps required to satisfy Eq. (3) decreases.

Among the proposed methods, the ANA method achieves the lowest false positive rate and the highest false negative rate. This is because a lot of nodes are given a higher interference ratio in the ANA method compared with the AINA and NINA methods, as described previously. When we compare the results of the AINA and NINA methods, the false positive rate becomes smaller and the false negative rate becomes higher for the NINA method when z is smaller than 0.9.

Figure 8 (b) shows the false negative rate and the false positive rate of the NINA method when the threshold B is changed. In the figure, the value of z is shown near to the results for $B = 3$. It can be seen that the false positive rate becomes lower and the false negative rate becomes higher as the threshold B increases. This is because the interference ratio of nodes becomes smaller as the threshold B decreases since the number of iteration steps required to satisfy Eq. (3) decreases.

In this subsection, we showed the accuracy of interference decision in the protocol interference model when z is varied. For network performance metrics, the number of time slots and the gateway throughput can be evaluated when $z = 1.0$ as described in Sect. 5.1. To evaluate network performance under $z < 1.0$, we should take into account situations that AMC mechanisms are applied and SINR is affected by Rayleigh fading. In addition, we should evaluate the network performance not only in terms of the number of time slots but also in terms of throughput at bit rates to handle varying throughput for each time slot. We plan to conduct these detailed evaluation under $z < 1.0$ as future work.

6. Conclusions

In this paper, we have investigated the relationship between interference decisions in the protocol interference and SINR models for TDMA-based wireless mesh networks. We proposed three methods (ANA, AINA and NINA) for adjusting the interference ratio parameter of the protocol interference model based on the SINR. Through simulation experiments, we found that accuracy of the protocol interference model is improved by up to 15% by adjusting the interference ratios of the protocol interference model using the NINA method.

In future work we will consider heterogeneous and dynamic cases where the transmission power of nodes is different and SINR is affected by Rayleigh fading and shadowing effects. We will also consider to apply AMC mechanisms and to evaluate detailed network performance in terms of throughput at bit rates. In addition, we should consider hop-based interference models, which are widely used in practical wireless networks, such as IEEE 802.16j networks. We plan to compare and investigate the relationships among the protocol interference, measurement-based SINR, hop-based interference models and actual interference through experimental evaluations.

Acknowledgments

References

[1] G. Kang, Y. Taniguchi, G. Hasegawa, and H. Nakano, "Extending the protocol inteference model considering SINR for wireless mesh networks," Proc. AICT 2011, pp.26–31, March 2011.

[2] I.F. Akyildiz, X. Wang, and W. Wang, "Wireless mesh networks: A survey," Comput. Netw., vol.47, no.4, pp.445–487, March 2005.

[3] B.N. Clark, C.J. Colbourn, and D.S. Johnson, "Unit disk graphs," Discrete Mathematics, vol.86, pp.165–177, Dec. 1990.

[4] M. Alicherry, R. Bhatia, and L. Lir, "Joint channel assignment and routing for throughput optimization in multi-radio wireless mesh networks," Proc. ACM MobiCom 2005, pp.58–72, Aug. 2005.

[5] V.S.A. Kumar, M.V. Marathe, S. Parthasarathy, and A. Srinivasan, "Algorithmic aspects of capacity in wireless networks," ACM SIGMETRICS Performance Evaluation Review, vol.33, pp.133–144, June 2005.

[6] Q. Chen, Q. Zhang, and Z. Niu, "A graph theory based opportunistic link scheduling for wireless ad hoc networks," IEEE Trans. Wireless Commun., vol.8, no.10, pp.5075–5085, Oct. 2009.

[7] W. Wang, Y. Wang, X.Y. Li, W.Z. Song, and O. Frieder, "Efficient interference-aware TDMA link scheduling for static wireless networks," Proc. ACM MobiCom 2006, pp.262–273, Sept. 2006.

[8] R. Ishii, G. Hasegawa, Y. Taniguchi, and H. Nakano, "Time slot assignment algorithms in IEEE 802.16 multi-hop relay networks," Proc. ICNS 2010, pp.265–270, March 2010.

[9] P. Gupta and P.R. Kumar, "The capacity of wireless networks," IEEE Trans. Inf. Theory, vol.46, no.2, pp.388–404, March 2000.

[10] Y. Shi, Y. Hou, J. Liu, and S. Kompella, "How to correctly use the protocol interference model for multi-hop wireless networks," Proc. ACM MobiHoc 2009, pp.239–248, May 2009.

[11] D. Son, B. Krishnamachari, and J. Heidemann, "Experimental study of concurrent transmission in wireless sensor networks," Proc. ACM SenSys 2006, pp.237–250, Nov. 2006.

[12] M. Zorzi and R.R. Rao, "Capture and retransmission control in mobile radio," IEEE J. Sel. Areas Commun., vol.12, no.8, pp.1289–1298, Oct. 1994.

[13] A. Chockalingam, M. Zorzi, L.B. Milstein, and P. Venkataram, "Performance of a wireless access protocol on correlated Rayeigh fading channels with capture," IEEE Trans. Commun., vol.46, no.5, pp.644–655, May 1998.

[14] V.S.A. Kumar, M.V. Marathe, S. Parthasarathy, and A. Srinivasan, "End-to-end packet-scheduling in wireless ad-hoc networks," Proc. SODA 2004, pp.1021–1030, Jan. 2004.

[15] G. Sharma, R.R. Mazumdar, and N.B. Shroff, "On the complexity of scheduling in wireless networks," Proc. ACM MobiCom 2006, pp.227–238, Sept. 2006.

[16] P. Chaporkar, K. Kar, X. Luo, and S. Sarkar, "Throughput and fairness guarantees through maximal scheduling in wireless networks," IEEE Trans. Inf. Theory, vol.54, no.2, pp.572–594, Feb. 2008.

[17] S. Yi, Y. Pei, and S. Kalyanaraman, "On the capacity improvement of ad hoc wireless networks using directional antennas," Proc. ACM MobiHoc 2003, pp.108–116, June 2003.

[18] R. Maheshwari, S. Jain, and S.R. Das, "A measurement study of interference modeling and scheduling in low-power wireless networks," Proc. ACM SenSys 2008, pp.141–154, Nov. 2008.

[19] X. Che, X. Liu, X. Ju, and H. Zhang, "Adaptive instantiation of the protocol interference model in mission-critical wireless networks," Proc. IEEE SECON 2010, pp.1–9, June 2010.

[20] H. Zhu and K. Lu, "On the interference modeling issues for coordinated distributed scheduling in IEEE 802.16 mesh networks," Proc. BROADNETS 2006, pp.1–10, Oct. 2006.

[21] F. Aurenhammer, "Voronoi diagrams–A survey of a fundamental geometric data structure," ACM Comput. Surv., vol.23, no.3, pp.345–405, Sept. 1991.

[22] L. Kleinrock and J. Silvester, "Spatial reuse in multihop packet radio networks," Proc. IEEE, pp.156–167, Jan. 1987.

Yoshiaki Taniguchi received his B.E., M.E. and Ph.D. degrees from Osaka University, Japan, in 2002, 2004 and 2008, respectively. Since 2008, he has been an Assistant Professor at the Cybermedia Center, Osaka University. His research interests include wireless sensor networks, wireless mesh networks, and object tracking systems. He is a member of IEEE and IPSJ.

Go Hasegawa received his M.E. and Ph.D. degrees from Osaka University, Japan, in 1997 and 2000, respectively. From 1997 to 2000, he was a Research Assistant at the Graduate School of Economics, Osaka University. He is currently an Associate Professor at the Cybermedia Center, Osaka University. His research is in the area of transport architecture for future high-speed networks. He is a member of IEEE.

Hirotaka Nakano received his B.E., M.E. and D.E. degrees in Electrical Engineering from The University of Tokyo, Japan, in 1972, 1974 and 1977, respectively. He joined NTT Laboratories in 1977 and has been engaged in research and development of videotex systems and multimedia-on-demand systems. He was an executive manager of the Multimedia Systems Laboratory at the NTT Human Interface Laboratories from 1995 to 1999. He was the head scientist of the Multimedia Laboratory at NTT DOCOMO until 2004 and is now a Professor at the Cybermedia Center, Osaka University. His research is in the area of ubiquitous networks. He is a member of IEEE and ITE.

Gyeongyeon Kang received her B.E. degree from Gyeongsang National University, Korea, in 2008, and her M.E. degree from Osaka University, Japan, in 2011. Her research interests include ubiquitous networking.